

# Combinatorial Drug Conjugation Enables Nanoparticle Dual-Drug Delivery

Santosh Aryal, Che-Ming Jack Hu, and Liangfang Zhang\*

**A** new approach to loading multiple drugs onto the same drug-delivery nanocarrier in a precisely controllable manner, by covalently preconjuga-ting multiple therapeutic agents through hydrolyzable linkers to form drug conjugates, is reported. In contrast to loading individual types of drugs separately, this drug-conjugates strategy enables the loading of multiple drugs onto the same carrier with a predefined stoichiometric ratio. The cleavable linkers allow the therapeutic activity of the individual drugs to be resumed after the drug conjugates are delivered into the target cells and unloaded from the delivery vehicle. As a proof of concept, the synthesis and characterization of paclitaxel–gemcitabine conjugates are demonstrated. The time-dependent hydrolysis kinetics and cytotoxicity of the combinatorial drug conjugates against human pancreatic cancer cells are examined. It is shown that the synthesized drug conjugates can be readily encapsulated into a lipid-coated polymeric drug-delivery nanoparticle, which significantly improves the cytotoxicity of the drug conjugates as compared to the free drug conjugates.

## Keywords:

- cancer therapy
- conjugation
- drug delivery
- lipid–polymer hybrids
- nanoparticles

## 1. Introduction

Combined therapy with two or more drugs provides a promising strategy to suppress cancer-drug resistance, as different drugs may attack cancer cells at varying stages of their growth cycles.<sup>[1]</sup> It has been reported in clinics that a variety of drug combinations can induce synergisms among them and prevent disease recurrence.<sup>[2,3]</sup> However, one major challenge of combinatorial therapy is to unify the pharmaco-

kinetics and cellular uptake of various drug molecules, which will allow the precise control of the dosage and scheduling of the multiple drugs, thereby maximizing the combinatorial effects. One of the most popular approaches to overcoming this challenge is to load multiple types of therapeutic agents onto a single drug-delivery vehicle and then concurrently deliver them to the sites of action.<sup>[4–7]</sup> Several drug-delivery systems, such as polymeric nanoparticles and liposomes, have shown the ability to co-deliver multiple drugs, but fine-controlling the comparative loading yield and release kinetics of the multiple-drug payloads remains an unmet need. Successfully addressing such a need will advance current nanomedicine research and enable more applications of combinatorial drug therapy.

Herein, we report a combinatorial drug-conjugation strategy to meet the aforementioned need by covalently conjugating multiple therapeutic agents through hydrolyzable linkers to form drug conjugates prior to loading the drugs onto a delivery vehicle. In contrast to loading individual types of drugs separately, this drug-conjugates approach enables multiple drugs to be loaded onto the same drug carrier with a predefined stoichiometric ratio. The cleavable linkers allow the therapeutic activity of the individual drugs to be resumed after the drug conjugates are delivered into the target cells and unloaded from the delivery vehicles. In this study, paclitaxel (PTXL) and

[\*] Prof. L. Zhang, Dr. S. Aryal  
Department of Nanoengineering  
University of California San Diego, La Jolla, CA 92093 (USA)  
E-mail: zhang@ucsd.edu  
Prof. L. Zhang, Dr. S. Aryal, C.-M. J. Hu  
Moores Cancer Center  
University of California San Diego, La Jolla, CA 92093 (USA)  
C.-M. J. Hu  
Department of Bioengineering  
University of California San Diego, La Jolla, CA 92093 (USA)

Supporting Information is available on the WWW under <http://www.small-journal.com> or from the author.

gemcitabine hydrochloride (GEM), two widely used anticancer chemotherapy drugs with completely different mechanisms of action, were chosen as model drugs.<sup>[8,9]</sup> The vast difference in hydrophobicity between PTXL (water insoluble) and GEM (water soluble) also makes them a pair of representative hydrophobic and hydrophilic drugs, which imposes some additional difficulties in the conjugation reaction as compared to two drugs with close hydrophobicity. We achieved the synthesis, characterization, and delivery of PTXL–GEM drug conjugates and evaluated their concentration and time-dependent cytotoxicity against human pancreatic cancer cells and their hydrolysis process. Note that the emphasis of this article is to present a unique chemical approach that enables nanoparticle-based combinatorial drug delivery, rather than demonstrating the synergistic effects between the two drugs chosen.

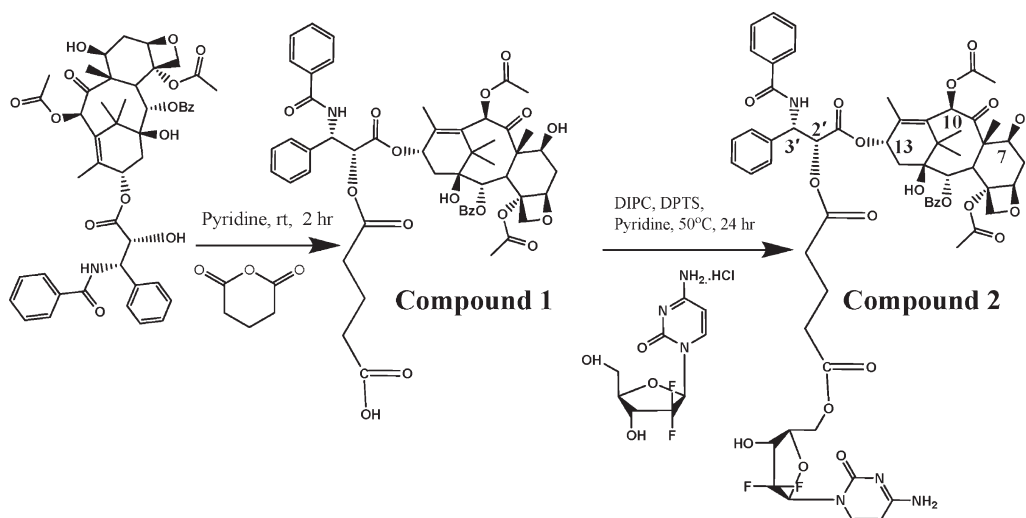
## 2. Results and Discussion

Figure 1 illustrates the synthesis scheme of the PTXL–GEM conjugate (compound **2**). We first took advantage of the steric hindrance structural chemistry of PTXL to selectively convert its 2'-hydroxyl group (2'-OH) to a carboxyl moiety (compound **1**). PTXL has three hydroxyl groups, of which two are secondary and one is tertiary. It has been reported that the tertiary hydroxyl group is highly hindered and unreactive.<sup>[10–12]</sup> The secondary hydroxyl group at the 7-position (7-OH) is less reactive than that at the 2'-position. Typically, one has to protect the 2'-OH to make any modification to the 7-OH group.<sup>[10,13]</sup> Here, we used glutaric anhydride (GA) in a reaction with PTXL in the presence of a catalytic amount of *N,N*-dimethylaminopyridine (DMAP) for 3 h at room temperature to selectively modify the 2'-OH group, which resulted in compound **1** as characterized in Figures S1–S3 (see Supporting Information). We observed that the reaction had to be limited to 3 h with a GA/PTXL molar ratio of 3:1 for the 2'-OH reaction, otherwise (longer reaction time or higher GA/PTXL ratio) a 7-OH reaction occurred. Compound **1** was then reacted with GEM using 1,3-diisopropyl carbodiimide (DIPC)

and 4-(*N,N*-dimethylamino)pyridinium-4-toluenesulfonate (DPTS), which resulted in the formation of compound **2**.

The production of compound **2** was first confirmed by <sup>1</sup>H NMR spectroscopy with all the characteristic peaks and their integration values of PTXL and GEM, respectively, as indicated in Figure 2A. The 2'-OH reaction was confirmed by the integration value of 14H for the resonance peaks at  $\delta = 2.7$ – $2.2$  ppm. These peaks correspond to the methyl protons of acetate groups at C-4 and C-10, the methylene protons at the C-14 position of the PTXL, and the methylene protons of the GA linker. The resonance at  $\delta = 2.7$ – $2.2$  ppm of unmodified PTXL was integrated as 8H, which increased to 14H after the conjugation with GA because of the addition of 6H of the methylene group from the GA moiety. In addition, the  $\delta = 4.4$  ppm peak of the protons at the C-7 position of PTXL remained intact during the conjugation. This further indicated that the PTXL–GA reaction only occurred at the 2'-OH group, as a downfield shifting of the C-7 proton would have appeared if the 7-OH reaction had taken place. In contrast, a significant downfield shifting from  $\delta = 4.7$  to 5.5 ppm was observed for the protons at the C-2' position. On the other hand, the use of GEM as its hydrochloride salt gives exclusive access to its hydroxyl group, which is thus prone to couple with the carboxyl group in the PTXL–GA to form an ester bond. In addition, it has been reported that DIPC and DPTS are effective esterification reagents with high reaction yield.<sup>[10]</sup> Furthermore, the chemical shift associated with the NH<sub>2</sub> protons of the pyrimidine ring at 9.0 ppm was intact after the reaction. This further confirms that the PTXL–GEM conjugation occurred via ester formation. The resulting compound **2** was further examined by high-resolution mass spectrometry to determine its mass and molecular formula. As shown in Figure 2B, the results were precisely consistent with the expected formula of PTXL–GEM conjugates.

As the ultimate goal of this research is to concurrently deliver two drugs to the same cancer cells for combinatorial therapy, it is crucial to ascertain that the linker bridging the drugs can be effectively hydrolyzed, thereby releasing the individual drugs to allow them to arrest cancer cells in their



**Figure 1.** Synthesis scheme of the paclitaxel (PTXL) and gemcitabine hydrochloride (GEM) conjugate (compound **2**).

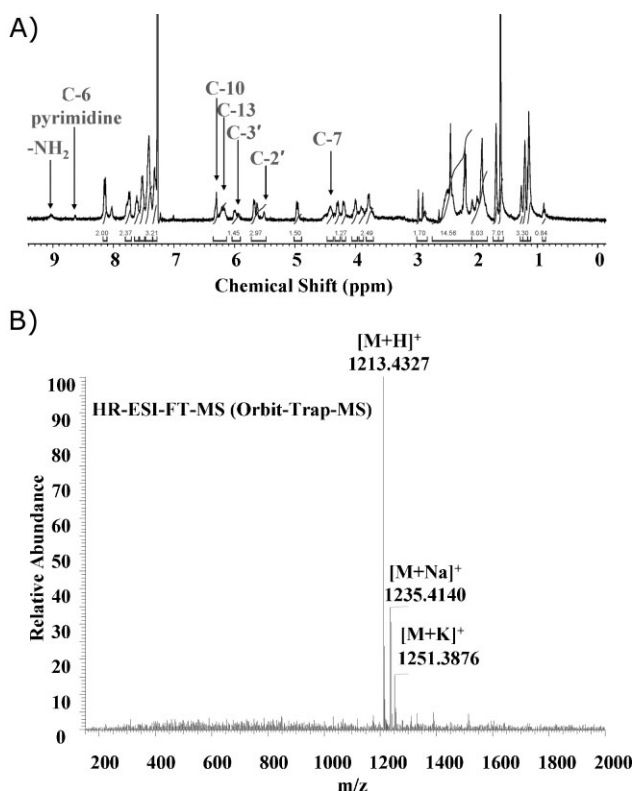


**Figure 2.** Characterization of PTXL–GEM conjugates by A)  $^1\text{H}$  NMR spectroscopy showing the characteristic protons, and B) high-resolution mass spectrometry determining the exact mass and corresponding molecular formula of the drug conjugates. HR-ESI-FT-MS = high-resolution electrospray-ionization Fourier transform mass spectrometry.

independent pathways. The hydrolysis of PTXL–GEM conjugates was evaluated and confirmed by high-performance liquid chromatography (HPLC) and high-resolution mass spectrometry. As shown in Figure 3A, the chromatogram clearly indicates that after 24 h of incubation in water/acetonitrile (75:25, v/v) solution at pH 7.4, a portion of the PTXL–GEM conjugate was hydrolyzed to free PTXL and free GEM with characteristic HPLC retention times of 6.2 and 1.8 min, respectively, which were confirmed by measuring the mass of the compounds collected at these two retention times (see Figures S4 and S5 in the Supporting Information for the corresponding mass spectra).

The formation of free PTXL and free GEM upon hydrolysis provided further evidence that PTXL–GEM conjugation occurred via the coupling of the hydroxyl and carboxyl groups to form an ester bond. If the reaction had occurred via amide formation between the  $\text{NH}_2$  group of the pyrimidine ring and the carboxyl group, free PTXL and free GEM would not have been released upon hydrolysis within only 24 h. We hypothesized that when these PTXL–GEM conjugates are delivered to target cells by a drug carrier through endocytosis, the conjugates can be hydrolyzed at a faster rate in the mild acidic endosomal environment ( $\text{pH} \approx 6$ ).<sup>[14–17]</sup> To test this hypothesis, we measured the hydrolysis kinetics of the PTXL–GEM conjugates at pH 6.0 and 7.4. As shown in Figure 3B, the hydrolysis rate was significantly faster in acidic environments (pH 6.0) than in neutral solution (pH 7.4). Nearly 80% of the

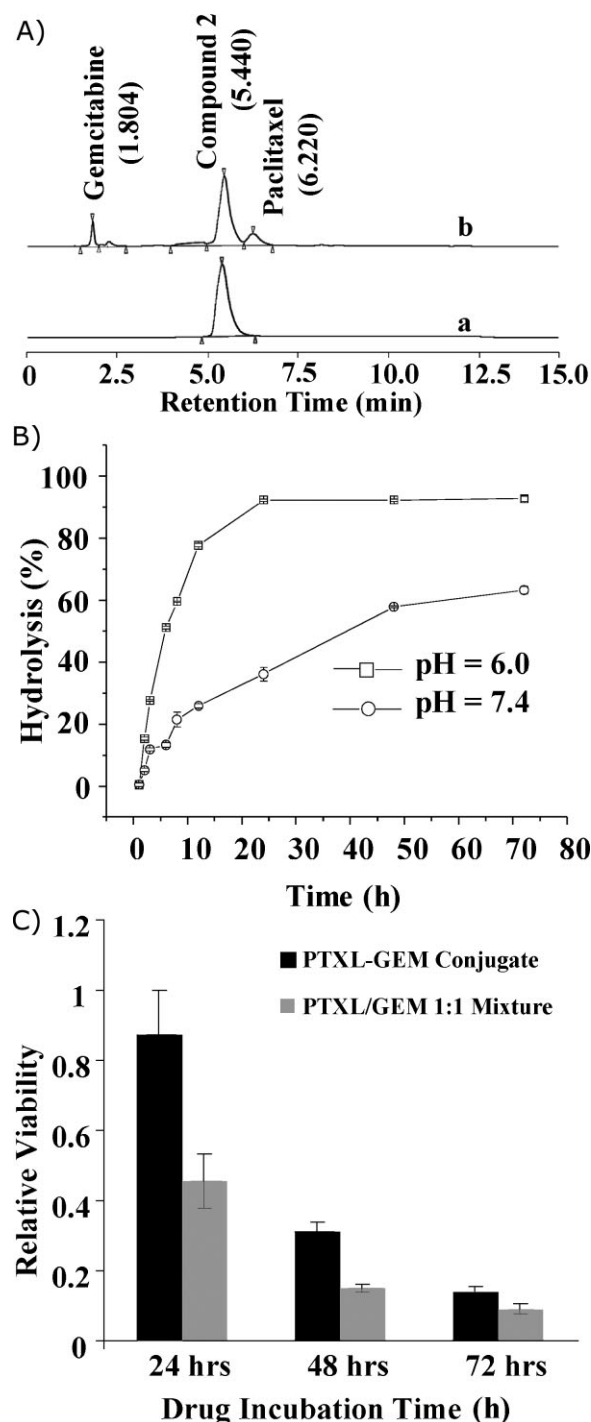


**Figure 3.** Hydrolysis and cellular cytotoxicity of PTXL–GEM conjugates. A) HPLC traces of PTXL–GEM conjugates a) before and b) after 24 h of incubation in water/acetonitrile (75:25, v/v) solution at pH 7.4. B) Hydrolysis kinetics of PTXL–GEM conjugates at pH 6.0 and 7.4. C) Time-dependent comparative cytotoxicity of PTXL–GEM conjugates with the corresponding mixture of free PTXL and free GEM at 100 nM concentration against XPA3 human pancreatic cancer cell line ( $n=8$ ).

drug conjugates were hydrolyzed to free PTXL and free GEM at pH 6.0 within the first 10 h, whereas less than 25% were cleaved at pH 7.4.

Next we examined the in vitro cellular cytotoxicity of free PTXL–GEM conjugates. As both PTXL and GEM are potent

chemotherapy drugs against pancreatic cancer, we chose human pancreatic cancer cell line XPA3 for this study.<sup>[18]</sup> Since it has been documented that the 2'-OH group is essential for the high cytotoxicity of PTXL,<sup>[13]</sup> it is natural to expect that the cytotoxicity profile of PTXL-GEM conjugates will rely on their hydrolysis process. To test this, we evaluated the cytotoxicity of the drug conjugates (100 nM concentration) at different hydrolysis durations, with a mixture of free PTXL (100 nM) and free GEM (100 nM) as a positive control. As shown in Figure 3C, a large cytotoxicity difference was observed between the drug conjugates and the free drug mixtures after 24 and 48 h of incubation, during which the drug conjugates were partially hydrolyzed. For example, the drug conjugates killed  $\approx 15\%$  of XPA3 cells whereas the drug mixtures killed  $\approx 55\%$  of the cells after 24 h of incubation. However, after 72 h of incubation, the cytotoxicity of the PTXL-GEM conjugates was nearly at the same level as that of the free PTXL and free GEM mixtures; over 80% of the cells were killed with both systems. This time-dependent cytotoxicity is consistent with the temporal hydrolysis profile of the PTXL-GEM conjugates at pH 7.4 measured by HPLC, as shown in Figure 3B. It is worth noting that small-molecule drugs such as PTXL, GEM, and PTXL-GEM conjugate can usually diffuse across the cell membranes to the inside of cells without going through the endocytosis mechanism. Therefore, the hydrolysis process of PTXL-GEM conjugates follows the pH = 7.4 profile when the drug conjugates are administered directly without using a drug-delivery vehicle.

After having demonstrated the formation of PTXL-GEM drug conjugates, their spontaneous hydrolysis to individual

drugs, and their cytotoxicity against human pancreatic cancer cell line XPA3, we next loaded the PTXL-GEM conjugates into a recently developed lipid-coated polymeric nanoparticle to validate the feasibility of using this preconjugation approach to enable nanoparticle dual-drug delivery. The PTXL-GEM conjugates were mixed with poly(lactic-co-glycolic acid) (PLGA) in an acetonitrile solution, which was subsequently added to an aqueous solution containing lipid and lipid-polyethylene glycol conjugates to prepare lipid-coated PLGA nanoparticles following a previously published protocol.<sup>[19]</sup>

Figure 4A shows a schematic representation of nanoparticles loaded with PTXL-GEM conjugates, which are spherical particles as imaged by scanning electron microscopy (SEM; Figure 4B). Dynamic light scattering (DLS) measurements showed that the resulting conjugate-loaded nanoparticles had a unimodal size distribution with an average hydrodynamic diameter of  $70 \pm 1.5$  nm (Figure 4C), which was consistent with the findings from the SEM image (Figure 3B). The surface zeta potential of the drug-loaded nanoparticles in water was about  $-53 \pm 2$  mV (Figure 4C). We further found that the size and surface zeta potential of the PTXL-GEM conjugate-loaded nanoparticles were similar to those of the corresponding empty nanoparticles, that is,  $70 \pm 1$  nm and  $-51 \pm 2$  mV, respectively. This suggests that the encapsulation of PTXL-GEM conjugates has a negligible effect on the formation of the lipid-coated polymeric nanoparticles.

The encapsulation yield and loading yield of PTXL-GEM conjugates in the nanoparticles were quantified by HPLC after dissolving the particles in organic solvents to free all encapsulated drugs. When the initial PTXL-GEM conjugate

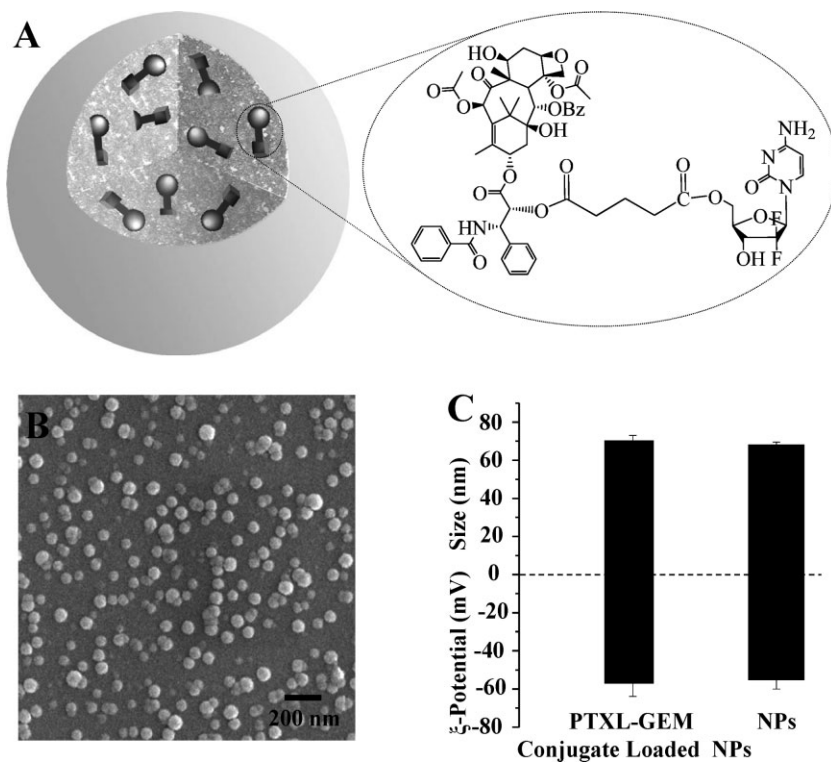


**Figure 4.** Characterization of PTXL-GEM conjugate-loaded lipid-coated polymeric nanoparticles (NPs). A) Schematic illustration of a PTXL-GEM conjugate-loaded nanoparticle. B) Representative SEM image of PTXL-GEM conjugate-loaded nanoparticles. C) Diameter and surface zeta potential of PTXL-GEM conjugate-loaded nanoparticles and empty nanoparticles measured by DLS.



input was 5, 10, and 15 wt% of the total nanoparticle weight, the drug encapsulation yield was  $22.8 \pm 2.0$ ,  $16.2 \pm 0.5$ , and  $10.8 \pm 0.7\%$ , respectively, which can be converted to the corresponding final drug loading yield of 1.1, 1.6, and 1.6 wt%, respectively (Figure 5A). Here, the drug encapsulation yield is defined as the weight ratio of the encapsulated drugs to the initial drug input. The drug loading yield is defined as the weight ratio of the encapsulated drugs to the entire drug-loaded nanoparticles including both excipients and bioactive drugs. It seemed that the maximum PTXL–GEM conjugate loading yield was about 1.6 wt% for the lipid-coated polymeric nanoparticles. This value can be converted to roughly 1700 PTXL–GEM drug conjugate molecules per nanoparticle, by calculations with the diameter of the nanoparticle (70 nm), the PLGA density ( $1.2 \text{ g mL}^{-1}$ ), and the molecular weight of the PTXL–GEM conjugate (1212 Da).

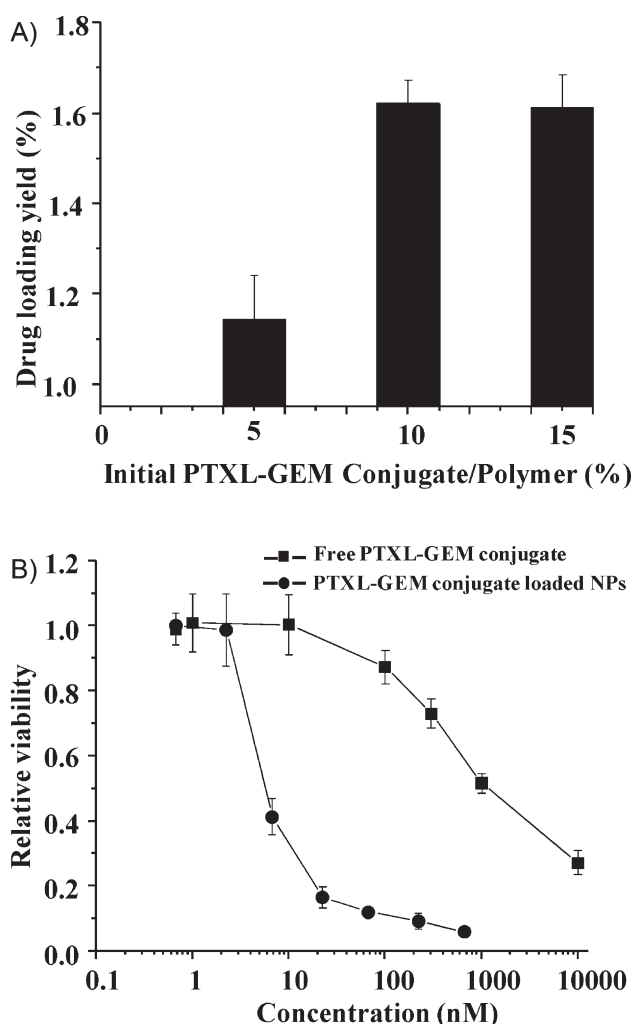


**Figure 5.** A) PTXL–GEM conjugate loading yield at various initial weight ratios of PTXL–GEM conjugates/excipient (PLGA polymer). B) Cellular cytotoxicity of PTXL–GEM conjugate-loaded nanoparticles and free PTXL–GEM conjugates (compound **2**) at various drug-conjugate concentrations against XPA3 human pancreatic cancer cell line. All samples were incubated with cells for 24 h, and the cells were subsequently washed and incubated in media for a total of 72 h before assessment of cell viability in each group ( $n = 8$ ).

The cytotoxicity of PTXL–GEM conjugate-loaded nanoparticles against XPA3 cell lines was then examined in comparison with free PTXL–GEM conjugates. Figure 5B summarizes the results of  $IC_{50}$  measurements of the conjugate-loaded nanoparticles and free PTXL–GEM conjugates for 24 h of incubation with the cancer cells. It was found that the  $IC_{50}$  value of the PTXL–GEM conjugates decreased by a factor of 200 for XPA3 cells after loading the drug conjugates into the lipid-coated polymeric nanoparticles. This enhanced cytotoxicity of the PTXL–GEM conjugates upon nanoparticle encapsulation can be explained, at least partially, by the fact that nanoparticle drug delivery can suppress cancer-drug resistance.<sup>[20,21]</sup> Small-molecule chemotherapy drugs that enter cells through either passive diffusion or membrane translocators are rapidly vacuumed out of the cells before they can take effect by transmembrane drug efflux pumps, such as P-glycoprotein (P-gp).<sup>[22]</sup> Drug-loaded nanoparticles, however, can partially bypass the efflux pumps as they are internalized through endocytosis.<sup>[23]</sup> Once engulfed by the plasma membrane, nanoparticles are transported by endosomal vesicles before unloading their drug payloads. Thus, drug molecules are released farther away from the membrane-bound drug efflux pumps and therefore are more likely to reach and interact with their targets. The endocytic uptake mechanism is particularly favorable to the combinatorial drug-delivery system presented in this study. The pH drop upon endosomal maturation into lysosomes<sup>[14]</sup> will subject the drug conjugates to a more acidic environment and more hydrolase enzymes,<sup>[24,25]</sup> which will facilitate the cleavage of the hydrolyzable linkers. Moreover, the degradation of the polymer PLGA will also contribute to lowering of the pH value surrounding the nanoparticles,<sup>[26]</sup> which can accelerate the hydrolysis process of the drug conjugates as well. The enhanced hydrolysis of the conjugate linkers may also be partially responsible for the near 200-fold cytotoxicity increase of PTXL–GEM conjugates after being encapsulated in the nanoparticles.

While the focus of this article is to report a novel chemical approach to loading two chemotherapy drugs into a single nanoparticle for combinatorial drug delivery, it would be interesting to compare the cytotoxicity of PTXL–GEM conjugate-loaded nanoparticles with that of a cocktail mixture of the same type of nanoparticles containing either free PTXL or free GEM. However, the vast difference in hydrophobicity (or solubility) between PTXL and GEM makes it practically impossible to load them into the same type of nanoparticle, such as the lipid-coated polymeric nanoparticles used in this study. These nanoparticles can encapsulate hydrophobic drugs such as PTXL with high encapsulation and loading yields but can barely encapsulate hydrophilic drugs such as GEM. In fact, the inability to load different drugs into the same type of nanoparticle represents a generic challenge to many pairs of drugs for combination therapy. The work presented herein may offer a new way to overcome this challenge.

### 3. Conclusions

We have demonstrated the conjugation of PTXL and GEM with a stoichiometric ratio of 1:1 via a hydrolyzable ester linker,

and have subsequently loaded the drug conjugates into lipid-coated polymeric nanoparticles. The cytotoxicity of the resulting combinatorial drug conjugates against human cancer cells was comparable to that of the corresponding free PTXL and GEM drug mixtures after the conjugates were hydrolyzed. The cytotoxicity of the drug conjugates was significantly improved after their encapsulation into drug-delivery nanoparticles. This work provides a new method to load dual drugs into the same drug-delivery vehicle in a precisely controllable manner, which holds great promise for suppressing cancer-drug resistance. A similar strategy may be generalized to other drug combinations. The synthesis of combinatorial drug conjugates with a broad range of stoichiometric ratios is currently ongoing in our laboratory.

## 4. Experimental Section

**Materials and instrumentation:** Paclitaxel (PTXL) and gemcitabine hydrochloride (GEM) were purchased from ChemiTek Co. and used without further purification. All other materials including solvents were purchased from Sigma-Aldrich Co., USA. A single-addition luminescence adenosine 5'-triphosphate (ATP) detection assay for cytotoxicity measurement was purchased from PerkinElmer Inc.  $^1\text{H}$  NMR spectra were recorded in  $\text{CDCl}_3$  using a Varian Mercury 400 MHz spectrometer. Electrospray ionization mass spectrometry (ESI-MS, Thermo LCQdeca spectrometer) and mass spectrometry (Thermo Fisher Scientific LTQ-XL Orbitrap spectrometer) were used to determine the mass and molecular formula of the compounds, respectively. Reversed-phase HPLC purification was performed on a Varian HPLC system equipped with a  $\mu$ -Bonapack C18 column ( $4.6 \times 150$  mm, Waters Associates, Inc.) with acetonitrile/water (50:50, v/v) as mobile phase. Thin-layer chromatography (TLC) measurements were carried out using precoated silica-gel HLF250 plates (Advenchen Laboratories, LLC, USA). DPTS was prepared by mixing saturated tetrahydrofuran (THF) solutions of DMAP (1 equiv) and *p*-toluenesulfonic acid monohydrate (1 equiv) at room temperature. The precipitate was isolated by filtration, washed three times with THF, and dried under vacuum.

**Synthesis of compound 1:** PTXL (5 mg,  $5.8 \mu\text{mol}$ ) and GA (2 mg,  $17.5 \mu\text{mol}$ ) were dissolved in dry pyridine (200  $\mu\text{L}$ ). DMAP ( $0.57 \mu\text{mol}$ ) dissolved in pyridine (10  $\mu\text{L}$ ) was added and the solution was stirred at room temperature for 3 h. The reaction was monitored by TLC using  $\text{CHCl}_3/\text{MeOH}$  (9.2:0.8, v/v) as eluent (product  $R_f = 0.42$ ). The complete disappearance of the starting PTXL ( $R_f = 0.54$ ) occurred after 3 h of reaction. Then the reaction was quenched by diluting the solution with dichloromethane (DCM), followed by extracting DMAP and pyridine with deionized (DI) water. The remaining DCM solution was concentrated and precipitated in hexane, which resulted in compound 1 as a white powder (5.1 mg, yield about 90%). NMR spectroscopy was carried out to characterize compound 1 (Figure S2, Supporting Information).  $^1\text{H}$  NMR ( $\text{CDCl}_3$ ):  $\delta = 1.14$  (s, 3H), 1.25 (s, 3H), 1.69 (s, 3H), 1.9–2.06 (broad (br), 7H), 2.16–2.27 (br, 4H), 2.2–2.7 (br, 14H), 3.82 (d, 1H), 4.21 (d, 1H), 4.32 (d, 1H), 4.48 (t, 1H), 5.0 (d, 1H), 5.5 (d, 1H), 5.69 (d, 1H), 6.0 (d, 1H), 6.3 (br, 2H), 7.09

(d, 1H), 7.3–7.4 (m, 7H), 7.5 (m, 3H), 7.6 (m, 1H), 7.74 (d, 2H), 8.13 (d, 2H), 8.6 ppm (s, 1H); ESI-MS (positive):  $m/z$ : 990.29  $[\text{M} + \text{Na}]^+$  (Figure S3, Supporting Information).

**Synthesis of PTXL–GEM conjugate (compound 2):** Compound 1 (5 mg,  $5.2 \mu\text{mol}$ ) was dissolved in dry DCM (0.5 mL) containing DPTS (4.6 mg,  $15.6 \mu\text{mol}$ ). A solution of GEM (1.5 mg,  $5.2 \mu\text{mol}$ ) dissolved in dry *N,N*-dimethylformamide (DMF; 0.5 mL) was added and the solution was stirred for 15 min. Then DIPC (5 mg,  $39 \mu\text{mol}$ ) in pyridine (0.1 mL) was added slowly to the solution and reaction was carried out at room temperature for 24 h. The reaction was monitored by TLC with  $\text{CHCl}_3/\text{MeOH}$  (9.2:0.8, v/v) as eluent (product  $R_f = 0.22$ ). The complete disappearance of the starting compound 1 ( $R_f = 0.42$ ) occurred after 24 h. The reaction was then quenched by diluting the solution with DCM, followed by extracting DPTS, DIPC, DMF, and pyridine with DI water. The remaining DCM solution was concentrated and precipitated in hexane, which resulted in compound 2 as a white powder (6.1 mg, yield about 86%). The crude product was purified by HPLC using acetonitrile/water (50:50, v/v) as eluent. NMR spectroscopy was carried out to characterize the produced compound 2 (Figure 2A).  $^1\text{H}$  NMR ( $\text{CDCl}_3$ ):  $\delta = 0.91$  (s, 1H), 1.14 (s, 3H), 1.22 (s, 3H), 1.27 (s, 3H), 1.62 (s, 7H), 1.67 (s, 3H), 1.9–1.2 (br, 8H), 2.2–2.7 (br, 14H), 2.89 (d, 2H), 3.7 (d, 2H), 3.85 (d, 2H), 3.9 (d, 1H), 4.32 (d, 1H), 4.48 (t, 1H), 5.0 (d, 1H), 5.5 (d, 1H), 5.69 (d, 1H), 6.0 (d, 1H), 6.3 (br, 3H), 7.28 (s, 3H), 7.4 (m, 5H), 7.5 (m, 3H), 7.6 (m, 1H), 7.74 (d, 2H), 8.13 (d, 2H), 8.75 (d, 1H), 9.1 ppm ( $\text{NH}_2$ , pyrimidine ring). The mass and molecular formula of compound 2 were determined by HR-ESI-FT-MS (orbit-trap MS, positive):  $m/z$ : 1213.4327  $[\text{M} + \text{H}]^+$ , 1235.4140  $[\text{M} + \text{Na}]^+$ ; calcd for  $\text{C}_{61}\text{H}_{66}\text{F}_2\text{N}_4\text{O}_{20}$ : 1213.4311; found: 1213.4327 (Figure 2B).

**Hydrolysis of PTXL–GEM conjugate (compound 2):** A hydrolysis study of PTXL–GEM conjugate was performed to confirm that it could be hydrolyzed to free PTXL and free GEM, and to measure the hydrolysis kinetics at different pH values. PTXL–GEM conjugate was incubated in aqueous solutions with a pH value of 6.0 or 7.4 at  $37^\circ\text{C}$ . At each predefined time interval, an aliquot of the conjugate solution was collected and subjected to HPLC (mobile phase: acetonitrile/water, 50:50, v/v) to determine the amount of free PTXL, free GEM, and the remaining PTXL–GEM conjugate.

**Preparation of drug-loaded nanoparticles:** Drug-loaded nanoparticles were prepared by a nanoprecipitation process. In a typical experiment, lecithin (0.12 mg, Alfa Aesar Co.) and 1,2-distearoyl-sn-glycero-3-phosphoethanolamine-*N*-[carboxy(polyethylene glycol)-2000] (0.259 mg, DSPE-PEG-COOH, Avanti Polar Lipids Inc.) was dissolved in 4% ethanol, homogenized to combine the components, and heated at  $68^\circ\text{C}$  for 3 min. PLGA (1 mg,  $M_n = 40$  kDa) and a calculated amount of drug dissolved in acetonitrile were added dropwise to the solution while heating and stirring. Then the vial was vortexed for 3 min followed by the addition of water (1 mL). The solution mixture was stirred at room temperature for 2 h, washed using an Amicon Ultra centrifugal filter (Millipore, Billerica, MA) with a molecular-weight cutoff of 10 kDa, and drug-loaded nanoparticles (1 mL) were collected. Bare nanoparticles were prepared similarly in the absence of drugs. The nanoparticle size and surface zeta potential were obtained from three repeat measurements by DLS (Malvern Zetasizer, ZEN 3600) with a backscattering angle of  $173^\circ$ . The morphology and particle

size were further characterized by SEM. Samples for SEM were prepared by dropping nanoparticle solution (5  $\mu$ L) onto a polished silicon wafer. After drying the droplet at room temperature overnight, the sample was coated with chromium and then imaged by SEM. The drug loading yield was determined by HPLC.

**Cellular viability assay:** The cytotoxicity of compound **2** and PTXL–GEM conjugate-loaded nanoparticles was assessed against XPA3 human pancreatic carcinoma cell line by using the ATP assay. First, cells were seeded ( $2 \times 10^4$ ) in 96-well plates and incubated for 24 h. Next, the medium was replaced with fresh medium (150  $\mu$ L) and incubated with a different concentration of compound **2** dissolved in dimethyl sulfoxide (DMSO). The final concentration of DMSO in each well was kept constant at 2%. The plates were then incubated for 72 h and measured by ATP reagents following a protocol provided by the manufacturer. Fresh cell medium with 2% DMSO was used as negative control. Similar procedures were applied to compare the cytotoxicity of 100 nm compound **2** with that of a mixture of free PTXL and GEM at the corresponding drug concentrations and incubation times of 24, 48, and 72 h. Here, the use of DMSO was only for solubilizing the free drugs. For the measurement of the cytotoxicity of PTXL–GEM conjugate-loaded nanoparticles, the experiments were carried out without using DMSO.

**Supporting Information:**  $^1\text{H}$  NMR spectra of the starting PTXL and intermediate compound **1**, and the mass spectra of compound **1**, free PTXL, and free GEM recovered from the hydrolyzed PTXL–GEM conjugate can be found in the Supporting Information.

## Acknowledgements

This work was supported by the National Institute of Health (grant U54CA119335) and the University of California San Diego.

- [1] J. Lehar, A. S. Krueger, W. Avery, A. M. Heilbut, L. M. Johansen, E. R. Price, R. J. Rickles, G. F. Short, 3rd, J. E. Staunton, X. Jin, M. S. Lee, G. R. Zimmermann, A. A. Borisy, *Nat. Biotechnol.* **2009**, *27*, 659–666.

- [2] F. Calabro, V. Lorusso, G. Rosati, L. Manzione, L. Frassinetti, T. Sava, E. D. Di Paula, S. Alonso, C. N. Sternberg, *Cancer* **2009**, *115*, 2652–2659.
- [3] H. M. McDaid, P. G. Johnston, *Clin. Cancer Res.* **1999**, *5*, 215–220.
- [4] S. Sengupta, D. Eavarone, I. Capila, G. Zhao, N. Watson, T. Kiziltepe, R. Sasisekharan, *Nature* **2005**, *436*, 568–572.
- [5] Y. Wang, S. Gao, W.-H. Ye, H. S. Yoon, Y.-Y. Yang, *Nat. Mater.* **2006**, *5*, 791–796.
- [6] L. Zhang, A. F. Radovic-Moreno, F. Alexis, F. X. Gu, P. A. Basto, V. Bagalkot, S. Jon, R. S. Langer, O. C. Farokhzad, *ChemMedChem* **2007**, *2*, 1268–1271.
- [7] F. Ahmed, R. I. Pakunlu, A. Brannan, F. Bates, T. Minko, D. E. Discher, *J. Controlled Release* **2006**, *116*, 150–158.
- [8] S. B. Horwitz, *Ann. Oncol.* **1994**, *5*(Suppl 6), S3–S6.
- [9] S. B. Horwitz, D. Cohen, S. Rao, I. Ringel, H. J. Shen, C. P. Yang, *J. Natl. Cancer Inst. Monogr.* **1993**, *15*, 55–61.
- [10] J. D. Gibson, B. P. Khanal, E. R. Zubarev, *J. Am. Chem. Soc.* **2007**, *129*, 11653–11661.
- [11] R. Tong, J. Cheng, *Angew. Chem.* **2008**, *120*, 4908–4912; *Angew. Chem. Int. Ed.* **2008**, *47*, 4830–4834.
- [12] R. Tong, J. Cheng, *J. Am. Chem. Soc.* **2009**, *131*, 4744–4754.
- [13] N. F. Magri, D. G. Kingston, *J. Nat. Prod.* **1988**, *51*, 298–306.
- [14] S. Modi, M. G. Swetha, D. Goswami, G. D. Gupta, S. Mayor, Y. Krishnan, *Nat. Nanotechnol.* **2009**, *4*, 325–330.
- [15] K. Remaut, B. Lucas, K. Braeckmans, J. Demeester, S. C. De Smedt, *J. Controlled Release* **2007**, *117*, 256–266.
- [16] X. Guo, F. C. Szoka, Jr., *Bioconjugate Chem.* **2001**, *12*, 291–300.
- [17] C. Masson, M. Garinot, N. Mignet, B. Wetzter, P. Mailhe, D. Scherman, M. Bessodes, *J. Controlled Release* **2004**, *99*, 423–434.
- [18] S. Kaushal, M. K. McElroy, G. A. Luiken, M. A. Talamini, A. R. Moossa, R. M. Hoffman, M. Bouvet, *J. Gastrointest. Surg.* **2008**, *12*, 1938–1950.
- [19] L. Zhang, J. M. Chan, F. X. Gu, J.-W. Rhee, A. Z. Wang, A. F. Radovic-Moreno, F. Alexis, R. Langer, O. C. Farokhzad, *ACS Nano* **2008**, *2*, 1696–1702.
- [20] C.-M. J. Hu, L. Zhang, *Curr. Drug Metab.* **2009**, *10*, 836–841.
- [21] E. M. Leslie, R. G. Deeley, S. P. Cole, *Toxicol. Appl. Pharmacol.* **2005**, *204*, 216–237.
- [22] M. M. Gottesman, *Annu. Rev. Med.* **2002**, *53*, 615–627.
- [23] J. Rejman, V. Oberle, I. S. Zuhom, D. Hoekstra, *Biochem. J.* **2004**, *377*, 159–169.
- [24] M. Masquelier, R. Baurain, A. Trouet, *J. Med. Chem.* **1980**, *23*, 1166–1170.
- [25] G. M. Dubowchik, M. A. Walker, *Pharmacol. Ther.* **1999**, *83*, 67–123.
- [26] H. Liu, E. B. Slamovich, T. J. Webster, *Int. J. Nanomedicine* **2006**, *1*, 541–545.

Received: April 15, 2010

Published online: June 17, 2010